

# Stable Quantum Monte Carlo Simulations for Entanglement Spectra of Interacting Fermions

Fakher F. Assaad

*Institut für Theoretische Physik und Astrophysik,  
Universität Würzburg, Am Hubland, D-97074 Würzburg, Germany*

(Dated: January 8, 2015)

We show that the two recently proposed methods to compute Renyi entanglement entropies in the realm of determinant quantum Monte Carlo methods for fermions are in principle equivalent, but differ in sampling strategies. The analogy allows to formulate a numerically stable calculation of the entanglement spectrum at strong coupling. We demonstrate the approach by studying static and dynamical properties of the entanglement hamiltonian across the interaction driven quantum phase transition between a topological insulator and quantum antiferromagnet in the Kane-Mele Hubbard model. The formulation is not limited to fermion systems and can readily be adapted to world-line based simulations of bosonic systems.

PACS numbers: 02.70.Ss, 03.67.-a, 71.10.-w, 73.43.-f

## I. INTRODUCTION

Consider a bipartition of a Hilbert space of a many body system in a state described by a density matrix  $\hat{\rho}$ . Tracing over the degrees of freedom of one partition defines a reduced density matrix. Its entropy provides a measure of the entanglement between the two partitions [1]. At zero temperature one generically expects the entanglement entropy to follow an area law [2]. Corrections to this law have the potential of revealing fundamental properties such as topological order [3–5] or the central charge for one-dimensional systems [6]. The logarithm of the reduced density matrix defines an entanglement Hamiltonian [7], the study of which has spurred substantial research [8–13]. The notion that it contains fundamental and universal information has emerged and has been critically discussed [14]. The aim of this article is to develop tools to study the properties on the entanglement Hamiltonian in the realm of quantum Monte Carlo (QMC) simulations for fermions.

For fermionic systems the calculation of the Renyi entanglement entropy has followed two different routes. One method builds on a replica idea with sampling based on a *swap* move [15, 16]. This approach was initially proposed for spin systems [15, 16] at zero and finite temperatures and then generalized to fermions in the realm of determinant [17] and continuous time [18] quantum Monte Carlo (QMC) methods. We will refer to this algorithm as the swap algorithm. The other approach put forward in Ref. [19] utilizes the fact that in auxiliary field algorithms [20] – which express the interacting system in terms of a sum of non-interacting problems, the density matrix can be formally written as a sum over gaussian operators [21]. We will refer to this algorithm as the gaussian approach. It is in principle simple to implement and allows for generalizations to compute entanglement spectra [22]. As pointed out in [17, 22] it suffers from an exponential growth of fluctuations in the strong coupling limit and when the subsystem size is *large*.

We will show that within the auxiliary field approach

both methods are equivalent, and merely correspond to different ways of carrying out the sampling. Since the swap algorithm is more stable than the gaussian one, the equivalence of the two methods shows how to stabilize the gaussian algorithm. As a consequence we are able to formulate a stable QMC algorithm allowing a detailed study of the entanglement Hamiltonian for fermion systems at strong coupling.

Here we will demonstrate the validity of the approach by studying a previously not accessible parameter region of the Kane-Mele Hubbard model [23–28]. In particular, we will concentrate on the correlation induced phase transition from a topological insulator to a quantum antiferromagnetic from the perspective of the entanglement spectrum both in the single particle and particle-hole sectors.

The article is organized as follows. In the next section we will show the equivalence of the swap and gaussian algorithms. Section III will use this equivalence to reformulate the proposed evaluation of the entanglement spectra of Ref. [22] in a numerically stable manner. Before concluding in Sec. V, we test our approach by studying the correlation driven quantum phase transition in the Kane-Mele Hubbard model from the perspective of the entanglement spectrum.

## II. EQUIVALENCE SWAP AND GAUSSIAN ALGORITHMS FOR THE $n^{\text{th}}$ RENYI ENTROPY.

Here we will start with the swap algorithm formulation of the  $n^{\text{th}}$  Renyi entropy and derive the gaussian algorithm of Ref. [19]. We consider a real space partitioning of the Hilbert space,  $\mathcal{H} = \mathcal{H}_A \otimes \mathcal{H}_B$ . To compute the  $n^{\text{th}}$  Renyi entropy,

$$S_n = -\frac{1}{n-1} \ln \text{Tr}_{\mathcal{H}_A} \hat{\rho}_A^n, \quad (1)$$

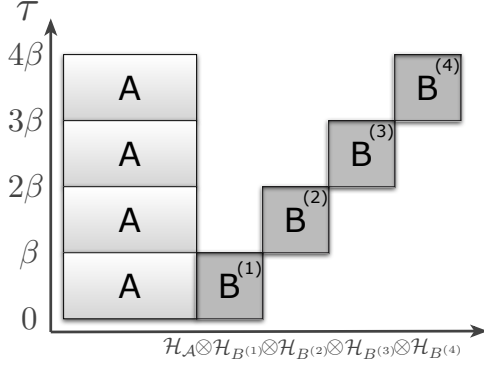


FIG. 1. Schematic view of the imaginary time propagation of the Hamiltonian  $\hat{H}(\tau)$  for the case  $n = 4$ . The Hamiltonian vanishes in the non-shaded regions.

with  $\hat{\rho}_A = \text{Tr}_{\mathcal{H}_B} \hat{\rho}$  and  $\hat{\rho}$  the density matrix, we consider the replicated Hilbert space:

$$\mathcal{H}_{\text{tot}} = \mathcal{H}_A \otimes \mathcal{H}_B^{(1)} \otimes \mathcal{H}_B^{(2)} \dots \mathcal{H}_B^{(n)}. \quad (2)$$

At  $n = 1$ ,  $\mathcal{H}_{\text{tot}}$  reduces to the original Hilbert space,  $\mathcal{H} = \mathcal{H}_A \otimes \mathcal{H}_B$ , and the Hamiltonian we will consider reads

$$\hat{H} = \sum_{\alpha} \hat{h}_A^{(\alpha)} \otimes \hat{h}_B^{(\alpha)}. \quad (3)$$

In the swap algorithm one expands the imaginary time propagation from  $\beta$  to  $n\beta$  (i.e.  $\tau \in [0, n\beta]$ ) and defines a time dependent Hamiltonian in the Hilbert space  $\mathcal{H}_{\text{tot}}$  as:

$$\hat{H}(\tau) = \sum_{r=1}^n \Theta[\tau - (r-1)\beta] \Theta[r\beta - \tau] \hat{H}^{(r)}. \quad (4)$$

$$\begin{aligned} \text{Tr}_{\mathcal{H}_{\text{tot}}} e^{-\beta \hat{H}^{(n)}} \dots e^{-\beta \hat{H}^{(1)}} &= \sum_{A_1 \dots A_n} \sum_{B_1 \dots B_n} \langle A_1, B_n^{(n)} | e^{-\beta \hat{h}^{(n)}} | A_n, B_n^{(n)} \rangle \langle A_n, B_{n-1}^{(n-1)} | e^{-\beta \hat{h}^{(n-1)}} | A_{n-1}, B_{n-1}^{(n-1)} \rangle \dots \times \\ &\langle A_2, B_1^{(1)} | e^{-\beta \hat{h}^{(1)}} | A_1, B_1^{(1)} \rangle = Z^n \sum_{A_1 \dots A_n} \langle A_1 | \hat{\rho}_A | A_n \rangle \langle A_n | \hat{\rho}_A | A_{n-1} \rangle \dots \langle A_2 | \hat{\rho}_A | A_1 \rangle = Z^n \text{Tr}_{\mathcal{H}_A} \hat{\rho}_A^n \end{aligned} \quad (9)$$

Note that the reduced density matrix  $\langle A | \hat{\rho}_A | A' \rangle = \frac{1}{Z} \sum_{B^{(r)}} \langle A, B^{(r)} | e^{-\beta \hat{h}^{(r)}} | A', B^{(r)} \rangle$  is independent on the choice of the replica. The partition function  $Z$  of the original Hamiltonian can be written as:

$$Z = \text{Tr}_{\mathcal{H}_{\text{tot}}} \left[ e^{-\beta \hat{H}^{(r)}} \right] d^{-(n-1)N_B}. \quad (10)$$

$d$  corresponds to the number of states per site ( $d = 4$  for the spin-1/2 Hubbard model) and  $N_B$  the number of sites in the partition  $B$  such that  $d^{(n-1)N_B}$  counts the number of states in the Hilbert space  $\mathcal{H} = \bigotimes_{r=1}^{n-1} \mathcal{H}_B^{(r)}$ . Hence, the factor  $d^{-(n-1)N_B}$  compensates the over count-

Here

$$\begin{aligned} \hat{H}^{(r)} &= \\ &\sum_{\alpha} \hat{h}_A^{(\alpha)} \otimes \hat{1}_B^{(1)} \dots \otimes \hat{1}_B^{(r-1)} \otimes \hat{h}_B^{(\alpha)} \otimes \hat{1}_B^{(r+1)} \dots \otimes \hat{1}_B^{(n)}. \end{aligned} \quad (5)$$

A schematic representation of this time evolution is given in Fig. 1. With this construction, one will show that:

$$\begin{aligned} \text{Tr}_{\mathcal{H}_A} \hat{\rho}_A^n &= \frac{1}{Z^n} \text{Tr}_{\mathcal{H}_{\text{tot}}} \mathcal{T} e^{-\int_0^{n\beta} d\tau \hat{H}(\tau)} \\ &\equiv \frac{1}{Z^n} \text{Tr}_{\mathcal{H}_{\text{tot}}} e^{-\beta \hat{H}^{(n)}} \dots e^{-\beta \hat{H}^{(1)}}. \end{aligned} \quad (6)$$

The above follows from writing the trace

$$\begin{aligned} \text{Tr}_{\mathcal{H}_{\text{tot}}} [\hat{O}] &= \\ &\sum_{A, B^{(1)}, \dots, B^{(n)}} \langle A, B^{(1)}, \dots, B^{(n)} | \hat{O} | A, B^{(1)}, \dots, B^{(n)} \rangle \end{aligned} \quad (7)$$

where  $A$  and  $B$  run over a complete set of orthonormal states of  $\mathcal{H}_A$  and  $\mathcal{H}_B$  respectively and by noting that:

$$\begin{aligned} \langle A, B^{(1)}, \dots, B^{(n)} | e^{-\beta \hat{H}^{(r)}} | A_1, B_1^{(1)}, \dots, B_1^{(n)} \rangle &= \\ \langle A, B^{(r)} | e^{-\beta \hat{h}^{(r)}} | A_1, B_1^{(r)} \rangle \prod_{\substack{i=1 \\ i \neq r}}^n \delta_{B^{(i)}, B_1^{(i)}}. \end{aligned} \quad (8)$$

Here  $\hat{H}^{(r)} \equiv \hat{h}^{(r)} \bigotimes_{i=1, i \neq r}^n \hat{1}_B^{(i)}$  such that  $\hat{h}^{(r)}$  corresponds to the Hamiltonian in Hilbert space  $\mathcal{H}_A \otimes \mathcal{H}_B^{(r)}$ . One can now explicitly compute the trace in Eq. (6) by inserting a complete set of states in  $\mathcal{H}_{\text{tot}}$  between each replica so as to obtain:

ing when computing the partition function of the original Hamiltonian by tracing over  $\mathcal{H}_{\text{tot}}$ . Note again that the partition function does not depend on the specific choice of the replica.

Thus,

$$\text{Tr}_{\mathcal{H}_A} \hat{\rho}_A^n = \quad (11)$$

$$\frac{\text{Tr}_{\mathcal{H}_{\text{tot}}} \left[ e^{-\beta \hat{H}^{(n)}} \dots e^{-\beta \hat{H}^{(1)}} \right]}{\text{Tr}_{\mathcal{H}_{\text{tot}}} \left[ e^{-\beta \hat{H}^{(n)}} \right] \dots \text{Tr}_{\mathcal{H}_{\text{tot}}} \left[ e^{-\beta \hat{H}^{(1)}} \right] d^{-n(n-1)N_B}}$$

We are now in the position to compute the Renyi en-

tropy with auxiliary field quantum Monte Carlo methods. Here, we will use the finite temperature algorithm [29, 30]. For a given replica, we can make use of the Trotter decomposition so as to write

$$e^{-\beta \hat{H}^{(r)}} = \prod_{\tau=1}^{L_\tau} e^{-\Delta\tau \hat{T}^{(r)}/2} e^{-\Delta\tau \hat{H}_U^{(r)}} e^{-\Delta\tau \hat{T}^{(r)}/2} + \mathcal{O}(\Delta\tau^2) \quad (12)$$

and the Hubbard Stratonovitch transformation

$$e^{-\Delta\tau \hat{H}_U^{(r)}} = \sum_{\mathbf{s}_\tau^{(r)}} e^{\hat{V}^{(r)}(\mathbf{s}_\tau^{(r)})}. \quad (13)$$

For each imaginary time and replica, we have a vector of Hubbard Stratonovitch fields,  $\mathbf{s}_\tau^{(r)}$ . It is important to remember that, by construction, the dimension of  $\mathbf{s}_\tau^{(r)}$  is identical to that of a single simulation at  $n = 1$ . For

the Hubbard model,  $\mathbf{s}_\tau^{(r)}$  corresponds to a vector of length  $N_A + N_B$  of Ising spins and we have used a transformation where the Ising field couples to the local density [31].  $\hat{T}^{(r)}$  and  $\hat{V}^{(r)}(\mathbf{s}_\tau^{(r)})$  are single particle operators which one can write as:

$$\hat{T}^{(r)} = \hat{\mathbf{c}}^\dagger T^{(r)} \hat{\mathbf{c}} \text{ and } \hat{V}^{(r)}(\mathbf{s}_\tau^{(r)}) = \hat{\mathbf{c}}^\dagger V^{(r)}(\mathbf{s}_\tau^{(r)}) \hat{\mathbf{c}}. \quad (14)$$

Here,  $\hat{\mathbf{c}}$  is a vector of fermionic annihilation operators running over all single particle states of the Hilbert space  $\mathcal{H}_{tot}$ . The imaginary time propagation now reads:

$$e^{-\beta \hat{H}^{(r)}} = \sum_{\mathbf{s}^{(r)}} \prod_{\tau=1}^{L_\tau} e^{-\Delta\tau \hat{T}^{(r)}/2} e^{\hat{V}^{(r)}(\mathbf{s}_\tau^{(r)})} e^{-\Delta\tau \hat{T}^{(r)}/2} \equiv \sum_{\mathbf{s}^{(r)}} \hat{U}_{\mathbf{s}^{(r)}}^{(r)} \quad (15)$$

where  $\mathbf{s}^{(r)}$  is a short hand notation for  $\mathbf{s}_1^{(r)} \cdots \mathbf{s}_{L_\tau}^{(r)}$ .

With the above, we can compute the Renyi entropy as:

$$\text{Tr}_{\mathcal{H}_A} \hat{\rho}_A^n = \frac{\sum_{\mathbf{s}^{(1)} \dots \mathbf{s}^{(n)}} \text{Tr}_{\mathcal{H}_{tot}} [\hat{U}_{\mathbf{s}^{(n)}}^{(n)} \cdots \hat{U}_{\mathbf{s}^{(1)}}^{(1)}]}{\sum_{\mathbf{s}^{(1)} \dots \mathbf{s}^{(n)}} \text{Tr}_{\mathcal{H}_{tot}} [\hat{U}_{\mathbf{s}^{(n)}}^{(n)}] \cdots \text{Tr}_{\mathcal{H}_{tot}} [\hat{U}_{\mathbf{s}^{(1)}}^{(1)}]} d^{-n(n-1)N_B}} \quad (16)$$

$\text{Tr}_{\mathcal{H}_A} \hat{\rho}_A^n$  corresponds to the ratio of two *partition functions*, defined on the same configuration space. Note that the symmetries which ensure the absence of sign problem for the original Hamiltonian can be used to prove the absence of sign problem for the numerator. For the Kane-Mele Hubbard model we refer the reader to [26, 27, 32] for a proof of the absence of sign problem at half-band

filling. The ratio in Eq. (16) can be computed with the swap algorithm described in [16]. This approach used to compute the Renyi entropies corresponds to the one adopted for bosonic systems and recently generalized to fermions [17]. To show the equivalence to the gaussian algorithm proposed in Ref. [19] and further developed in Ref. [22] to access entanglement spectrum we can rewrite Eq. (16) as:

$$\text{Tr}_{\mathcal{H}_A} \hat{\rho}_A^n = \sum_{\mathbf{s}^{(1)}, \dots, \mathbf{s}^{(n)}} P(\mathbf{s}^{(1)}, \dots, \mathbf{s}^{(n)}) \langle \langle \hat{O} \rangle \rangle_{\mathbf{s}^{(1)} \dots \mathbf{s}^{(n)}} \quad (17)$$

where

$$P(\mathbf{s}^{(1)}, \dots, \mathbf{s}^{(n)}) = \frac{\text{Tr}_{\mathcal{H}_{tot}} [\hat{U}_{\mathbf{s}^{(n)}}^{(n)}] \cdots \text{Tr}_{\mathcal{H}_{tot}} [\hat{U}_{\mathbf{s}^{(1)}}^{(1)}]}{\sum_{\mathbf{s}^{(1)} \dots \mathbf{s}^{(n)}} \text{Tr}_{\mathcal{H}_{tot}} [\hat{U}_{\mathbf{s}^{(n)}}^{(n)}] \cdots \text{Tr}_{\mathcal{H}_{tot}} [\hat{U}_{\mathbf{s}^{(1)}}^{(1)}]} \quad (18)$$

and

$$\langle \langle \hat{O} \rangle \rangle_{\mathbf{s}^{(1)} \dots \mathbf{s}^{(n)}} = \frac{\text{Tr}_{\mathcal{H}_{tot}} [\hat{U}_{\mathbf{s}^{(n)}}^{(n)} \cdots \hat{U}_{\mathbf{s}^{(1)}}^{(1)}]}{\text{Tr}_{\mathcal{H}_{tot}} [\hat{U}_{\mathbf{s}^{(n)}}^{(n)}] \cdots \text{Tr}_{\mathcal{H}_{tot}} [\hat{U}_{\mathbf{s}^{(1)}}^{(1)}]} d^{-n(n-1)N_B} \quad (19)$$

The probability distribution  $P(\mathbf{s}^{(1)}, \dots, \mathbf{s}^{(n)})$  is sampled by carrying out  $n$ -independent simulations of the original Hamiltonian. Our task is now to show that  $\langle \langle \hat{O} \rangle \rangle_{\mathbf{s}^{(1)} \dots \mathbf{s}^{(n)}}$

reduces to Grover's form [19] for the calculation of the Renyi entropy.

### A. The $n = 2$ case.

At  $n = 2$  one can follow a pedestrian path and compute the ratio of the two fermionic determinants. We will sketch the calculation under the assumption that  $\hat{U}_{\mathbf{s}^{(r)}}^{(r)}$  factorizes into spin-up and spin-down components such that we can only concentrate on the orbital degrees of freedom. Let  $P_A$  be a  $(N_A + 2N_B) \times (N_A + 2N_B)$  matrix with

$$(P_A)_{\mathbf{i}, \mathbf{j}} = \begin{cases} \delta_{\mathbf{i}, \mathbf{j}} & \text{if } \mathbf{i} \in A \\ 0 & \text{otherwise} \end{cases} \quad (20)$$

Here  $\mathbf{i}$  and  $\mathbf{j}$  run over all the single particle Wannier states of the Hilbert space  $\mathcal{H}_A \otimes \mathcal{H}_B \otimes \mathcal{H}_{B'}$ , and  $\mathbf{i} \in A$  states that Wannier state  $\mathbf{i}$  belongs to  $\mathcal{H}_A$ . Clearly  $P_A$  is a projector, and we will define similar quantities  $P_B$  and  $P_{B'}$ . Note that  $P_A, P_B$  and  $P_{B'}$  are projectors on orthogonal spaces such that for example  $P_A P_B = 0$ . For a given spin sector with  $d = 2$  the integration over the

fermionic degrees of freedom gives [29, 33]:

$$\langle \langle \hat{O} \rangle \rangle_{\mathbf{s}^{(1)}, \mathbf{s}^{(2)}} = \frac{\det \left[ 1 + U_{\mathbf{s}^{(2)}}^{(2)} U_{\mathbf{s}^{(1)}}^{(1)} \right]}{\det \left[ 1 + U_{\mathbf{s}^{(2)}}^{(2)} \right] \det \left[ 1 + U_{\mathbf{s}^{(1)}}^{(1)} \right] 2^{-2N_B}} \quad (21)$$

In the above equation we have defined

$$U_{\mathbf{s}^{(r)}}^{(r)} = \prod_{\tau=1}^{L_\tau} e^{-\Delta\tau T^{(r)}/2} e^{V^{(r)}(\mathbf{s}_\tau^{(r)})} e^{-\Delta\tau T^{(r)}/2}. \quad (22)$$

Since the equal time Green function [33] in each replica reads,

$$G_{\mathbf{s}^{(r)}}^{(r)} = \left[ 1 + U_{\mathbf{s}^{(r)}}^{(r)} \right]^{-1} \quad (23)$$

we can see, after some algebra, that

$$\langle \langle \hat{O} \rangle \rangle_{\mathbf{s}^{(1)}, \mathbf{s}^{(2)}} = \det \left[ P_A \left( 2G_{\mathbf{s}^{(2)}}^{(2)} P_A G_{\mathbf{s}^{(1)}}^{(1)} - G_{\mathbf{s}^{(2)}}^{(2)} - G_{\mathbf{s}^{(1)}}^{(1)} + 1 \right) P_A + P_B + P_{B'} \right]. \quad (24)$$

Since  $P_A, P_B$  and  $P_{B'}$  are orthogonal projectors, the above determinant reduces to the determinant of the  $N_A \times N_A$  matrix  $\det \left[ (G_A^{(2)} - 1)(G_A^{(1)} - 1) + G_A^{(2)} G_A^{(1)} \right]$  where  $G_A^{(r)}$  corresponds to the Green function  $G_{\mathbf{s}^{(r)}}^{(r)}$  restricted to Wannier states within  $\mathcal{H}_A$ . The above is nothing but the equation put forward by Grover [19].

### B. The general case.

To show the equivalence for the  $n^{\text{th}}$  Renyi entropy one notes that  $\hat{U}_{\mathbf{s}^{(r)}}^{(r)}$  acts non trivially in the Hilbert space  $\mathcal{H}_A \otimes \mathcal{H}_B^{(r)}$ . Hence,

$$\hat{U}_{\mathbf{s}^{(r)}}^{(r)} = \hat{u}_{\mathbf{s}^{(r)}}^{(r)} \bigotimes_{\substack{i=1 \\ i \neq r}}^n \hat{1}_B^{(i)} \quad (25)$$

The same calculation which leads to Eq. (6) gives

$$\text{Tr}_{\mathcal{H}_{\text{tot}}} \left[ \hat{U}_{\mathbf{s}^{(n)}}^{(n)} \cdots \hat{U}_{\mathbf{s}^{(1)}}^{(1)} \right] = \text{Tr}_{\mathcal{H}_A} \left[ \tilde{\rho}_A(\mathbf{s}^{(n)}) \cdots \tilde{\rho}_A(\mathbf{s}^{(1)}) \right] \quad (26)$$

where

$$\tilde{\rho}_A(\mathbf{s}^{(r)}) = \text{Tr}_{\mathcal{H}_B^{(r)}} \left[ \hat{u}_{\mathbf{s}^{(r)}}^{(r)} \right]. \quad (27)$$

Using the relation

$$\text{Tr}_{\mathcal{H}_{\text{tot}}} \left[ \hat{U}_{\mathbf{s}^{(r)}}^{(r)} \right] = \text{Tr}_{\mathcal{H}_A \otimes \mathcal{H}_B^{(r)}} \left[ \hat{u}_{\mathbf{s}^{(r)}}^{(r)} \right] d^{(n-1)N_B} \quad (28)$$

one obtains:

$$\langle \langle \hat{O} \rangle \rangle_{\mathbf{s}^{(1)} \dots \mathbf{s}^{(n)}} = \text{Tr}_{\mathcal{H}_A} \left[ \hat{\rho}_A(\mathbf{s}^{(n)}) \cdots \hat{\rho}_A(\mathbf{s}^{(1)}) \right] \quad (29)$$

with

$$\hat{\rho}_A(\mathbf{s}^{(r)}) = \frac{\text{Tr}_{\mathcal{H}_B^{(r)}} \left[ \hat{u}_{\mathbf{s}^{(r)}}^{(r)} \right]}{\text{Tr}_{\mathcal{H}_A \otimes \mathcal{H}_B^{(r)}} \left[ \hat{u}_{\mathbf{s}^{(r)}}^{(r)} \right]}. \quad (30)$$

$\hat{\rho}_A(\mathbf{s}^{(r)})$  is an operator acting in  $\mathcal{H}_A$ . For a fixed Hubbard Stratonovitch configuration,  $\hat{u}_{\mathbf{s}^{(r)}}^{(r)}$  is a single particle propagator such that Wick's theorem applies. As pointed out in [19] it has a Gaussian representation uniquely defined by the Green function  $G_A^{(r)}$  given at the end of the previous sub-section. In particular:

$$\hat{\rho}_A(\mathbf{s}^{(r)}) = \det \left( 1 - G_A^{(r)} \right) e^{-\hat{\mathbf{a}}^\dagger \ln \left( \frac{1 - G_A^{(r)}}{G_A^{(r)}} \right) \hat{\mathbf{a}}} \quad (31)$$

where  $\hat{\mathbf{a}}$  is a vector of fermionic annihilation operators running over all single particle states of the Hilbert space  $\mathcal{H}_A$ . Taking the trace over  $\mathcal{H}_A$  gives:

$$\langle \langle \hat{O} \rangle \rangle_{\mathbf{s}^{(1)} \dots \mathbf{s}^{(n)}} = \prod_{r=1}^n \det \left( 1 - G_A^{(r)} \right) \det \left( 1 + \prod_{r=1}^n \frac{G_A^{(r)}}{1 - G_A^{(r)}} \right) \quad (32)$$

which is nothing but the general result of Ref. [19].

### III. ENTANGLEMENT SPECTRA

In Ref. [22] we proposed to compute the entanglement spectrum by considering the replica time displaced correlation function:

$$S_O^E(\tau_E) \equiv \langle \hat{O}^\dagger(\tau_E) \hat{O} \rangle_A \equiv \frac{\text{Tr}_{\mathcal{H}_A} \left[ \hat{\rho}_A^{(n-\tau_E)} \hat{O}^\dagger \hat{\rho}_A^{\tau_E} \hat{O} \right]}{\text{Tr}_{\mathcal{H}_A} [\hat{\rho}_A^n]}, \quad (33)$$

$$S_O^E(\tau_E) = \frac{\sum_{\mathbf{s}^{(1)} \dots \mathbf{s}^{(n)}} P(\mathbf{s}^{(1)}, \dots, \mathbf{s}^{(n)}) \text{Tr}_{\mathcal{H}_A} \left[ \hat{\rho}_A(\mathbf{s}^{(n)}) \dots \hat{\rho}_A(\mathbf{s}^{(\tau_E+1)}) \hat{O}^\dagger \hat{\rho}_A(\mathbf{s}^{(\tau_E)}) \dots \hat{\rho}_A(\mathbf{s}^{(1)}) \hat{O} \right]}{\sum_{\mathbf{s}^{(1)} \dots \mathbf{s}^{(n)}} P(\mathbf{s}^{(1)}, \dots, \mathbf{s}^{(n)}) \text{Tr}_{\mathcal{H}_A} [\hat{\rho}_A(\mathbf{s}^{(n)}) \dots \hat{\rho}_A(\mathbf{s}^{(1)})]}. \quad (35)$$

Sampling over  $n$ -independent simulations generates configurations distributed according to  $P(\mathbf{s}^{(1)}, \dots, \mathbf{s}^{(n)})$  such that in principle one can compute numerator and denominator within a single simulation to provide an estimate of the replica time displaced correlation function. This approach works at weak coupling but fails in the strong coupling limit due to fluctuations. Essentially, one is sampling the wrong distribution,  $P(\mathbf{s}^{(1)}, \dots, \mathbf{s}^{(n)})$  and re-weighting with the factor

for an operator  $\hat{O} \in \mathcal{H}_A$ . Here  $\tau_E$  and  $n$  are integers with  $\tau_E < n$ . Within the gaussian approach [19] we can use the representation of the reduced density matrix,

$$\hat{\rho}_A = \sum_{\mathbf{s}} P(\mathbf{s}) \hat{\rho}_A(\mathbf{s}), \quad (34)$$

introduce  $n$  replicas and obtain:

$\text{Tr}_{\mathcal{H}_A} [\hat{\rho}_A(\mathbf{s}^{(n)}) \dots \hat{\rho}_A(\mathbf{s}^{(1)})]$  which accounts for correlations between the replicas. Since one can show that the later quantity is positive it was proposed in [22] to sample directly,  $P(\mathbf{s}^{(1)}, \dots, \mathbf{s}^{(n)}) \text{Tr}_{\mathcal{H}_A} [\hat{\rho}_A(\mathbf{s}^{(n)}) \dots \hat{\rho}_A(\mathbf{s}^{(1)})]$  so as to access the strong coupling regime.

One can achieve this by using the above presented mapping between the gaussian and replica methods. In fact in the extended Hilbert space, one will see that:

$$S_O^E(\tau_E) = \frac{\sum_{\mathbf{s}^{(1)} \dots \mathbf{s}^{(n)}} \text{Tr}_{\mathcal{H}_{tot}} \left[ \hat{U}_{\mathbf{s}^{(n)}}^{(n)} \dots \hat{U}_{\mathbf{s}^{(\tau_E+1)}}^{(\tau_E+1)} \hat{O}^\dagger \hat{U}_{\mathbf{s}^{(\tau_E)}}^{(\tau_E)} \dots \hat{U}_{\mathbf{s}^{(1)}}^{(1)} \hat{O} \right]}{\sum_{\mathbf{s}^{(1)} \dots \mathbf{s}^{(n)}} \text{Tr}_{\mathcal{H}_{tot}} \left[ \hat{U}_{\mathbf{s}^{(n)}}^{(n)} \dots \hat{U}_{\mathbf{s}^{(1)}}^{(1)} \right]} \quad (36)$$

such that:

$$\langle O(\tau_E) O \rangle_A = \sum_{\mathbf{s}^{(1)} \dots \mathbf{s}^{(n)}} \tilde{P}(\mathbf{s}^{(1)} \dots \mathbf{s}^{(n)}) \langle \langle O(\tau_E) O \rangle \rangle_{\mathbf{s}^{(1)} \dots \mathbf{s}^{(n)}} \quad (37)$$

with

$$\tilde{P}(\mathbf{s}^{(1)} \dots \mathbf{s}^{(n)}) = \frac{\text{Tr}_{\mathcal{H}_{tot}} \left[ \hat{U}_{\mathbf{s}^{(n)}}^{(n)} \dots \hat{U}_{\mathbf{s}^{(1)}}^{(1)} \right]}{\sum_{\mathbf{s}^{(1)} \dots \mathbf{s}^{(n)}} \text{Tr}_{\mathcal{H}_{tot}} \left[ \hat{U}_{\mathbf{s}^{(n)}}^{(n)} \dots \hat{U}_{\mathbf{s}^{(1)}}^{(1)} \right]} \quad (38)$$

and

$$\langle \langle O(\tau_E) O \rangle \rangle_{\mathbf{s}^{(1)} \dots \mathbf{s}^{(n)}} = \frac{\text{Tr}_{\mathcal{H}_{tot}} \left[ \hat{U}_{\mathbf{s}^{(n)}}^{(n)} \dots \hat{U}_{\mathbf{s}^{(\tau_E+1)}}^{(\tau_E+1)} \hat{O}^\dagger \hat{U}_{\mathbf{s}^{(\tau_E)}}^{(\tau_E)} \dots \hat{U}_{\mathbf{s}^{(1)}}^{(1)} \hat{O} \right]}{\text{Tr}_{\mathcal{H}_{tot}} \left[ \hat{U}_{\mathbf{s}^{(n)}}^{(n)} \dots \hat{U}_{\mathbf{s}^{(1)}}^{(1)} \right]}. \quad (39)$$

The above corresponds to a *standard* calculation of an imaginary time displaced correlation function in the extended Hilbert space at temperature  $n\beta$  albeit with an imaginary time dependent Hamiltonian. This quantity can readily be implemented in standard auxiliary field

finite temperature quantum Monte-Carlo methods. The above formulation is however not restricted to fermions. In fact, it carries over to bosonic systems amenable to stochastic simulations within, for example, the stochastic series expansion algorithm [34].

### IV. RESULTS

To illustrate the fact that we are able to access the strong coupling regime, we consider the interaction driven quantum phase transition in the Kane-Mele Hubbard model. The model is defined on the Honeycomb lattice. Using the spinor notation  $\hat{\mathbf{c}}_i^\dagger = (\hat{c}_{i\uparrow}^\dagger, \hat{c}_{i\downarrow}^\dagger)$  it reads

$$\hat{H}_{KMU} = \sum_{\mathbf{i}, \mathbf{j}} \hat{c}_{\mathbf{i}}^\dagger [t_{\mathbf{ij}} + i \lambda_{\mathbf{ij}} \cdot \boldsymbol{\sigma}] \hat{c}_{\mathbf{j}} + \frac{U}{2} \sum_{\mathbf{i}} \left( \hat{c}_{\mathbf{i}}^\dagger \hat{c}_{\mathbf{i}} - 1 \right)^2. \quad (40)$$

The hopping matrix takes non-vanishing values,  $-t$ , between nearest neighbors of the honeycomb lattice,  $\mathbf{i} - \mathbf{j} = \pm \boldsymbol{\delta}_1, \pm \boldsymbol{\delta}_2, \pm \boldsymbol{\delta}_3$  (see Fig. 2) and the intrinsic spin-

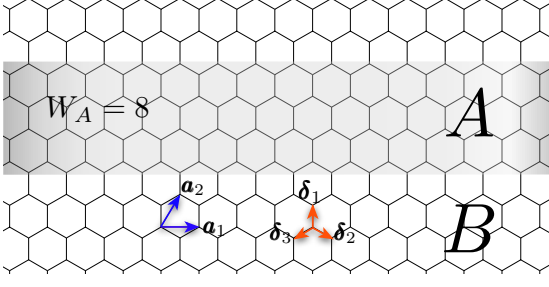


FIG. 2. Honeycomb lattice. For an  $L \times L$  lattice, we consider periodic boundaries:  $\mathbf{c}_{\mathbf{i}+L\mathbf{a}_1} = \mathbf{c}_{\mathbf{i}}$  and  $\mathbf{c}_{\mathbf{i}+L\mathbf{a}_2} = \mathbf{c}_{\mathbf{i}}$ . The real space partitioning breaks translation symmetry in the  $\mathbf{a}_2$  direction but not along  $\mathbf{a}_1$ .

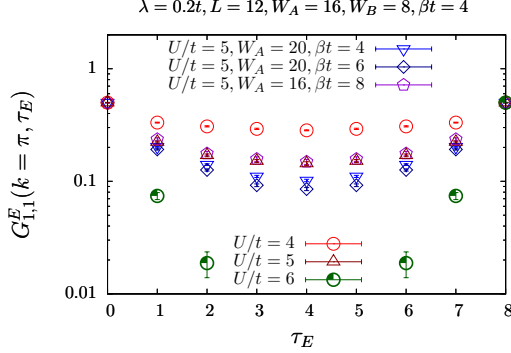


FIG. 3. Entanglement single particle Green function. Here we concentrate on the time reversal symmetric momentum  $k = \pi$  and orbital  $m = 1$  lying on the boundary of subsystem A.

orbit term is given by

$$\lambda_{ij} = \lambda \begin{cases} \frac{(\mathbf{i}-\mathbf{r}) \times (\mathbf{r}-\mathbf{j})}{|(\mathbf{i}-\mathbf{r}) \times (\mathbf{r}-\mathbf{j})|} & \text{if } \mathbf{i}, \mathbf{j} \text{ are n.n.n.} \\ 0 & \text{otherwise} \end{cases}, \quad (41)$$

where  $\mathbf{r}$  is the intermediate site involved in the next nearest neighbor (n.n.n.) hopping process from site  $\mathbf{i}$  to  $\mathbf{j}$ . At  $\lambda = 0.2t$  the model shows a zero temperature phase transition between a quantum spin Hall state and a quantum antiferromagnetic at  $U_c/t = 5.71(2)$  [35]. The quantum phase transition is well understood and belongs to the 3D XY universality class. Here, we show that we can detect this phase transition in the entanglement spectrum. In the absence of interactions the entanglement Hamiltonian is adiabatically linked to the original one such that both have the same topological properties [11, 12]. Thereby the entanglement Hamiltonian corresponding to a real space partitioning of the system should show edge states.

Fig. 3 shows the single particle entanglement replica

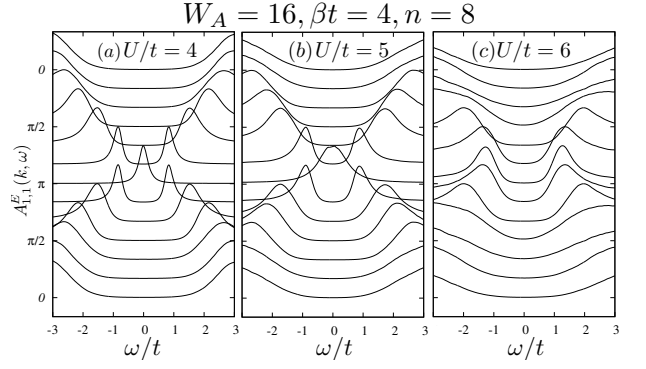


FIG. 4. Entanglement spectral function as a function of the Hubbard  $U$ . For each  $k$ -point the sum rule  $\int d\omega A_{1,1}^E(k, \omega) = 1$  holds. In the plot, we have normalized the peak height to unity.

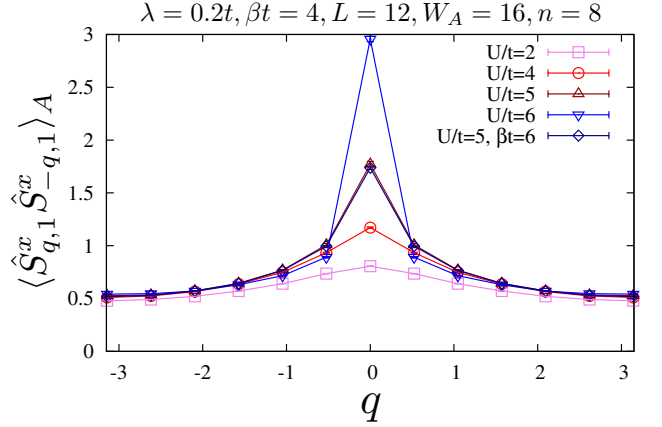


FIG. 5. x-component of the spin-spin correlation function taken on the edge of subsystem A corresponding to orbital index  $m = 1$ .

time displaced Green function,

$$G_{m,m'}^E(k, \tau_E) = \frac{1}{2} \sum_{\sigma} \langle \hat{a}_{k,m,\sigma}^\dagger(\tau_E) \hat{a}_{k,m',\sigma} \rangle_A. \quad (42)$$

The real space cut we consider is translationally invariant in the  $\mathbf{a}_1$  lattice direction. Thereby,  $k = \mathbf{k} \cdot \mathbf{a}_1$  is a good quantum number which we can use to classify the data. The label  $m$  is an *orbital* index running across the width,  $W_A$ , of the cut. In Fig. 3 we consider a  $12 \times 12$  lattice with  $n = 8$  replicas,  $W_A = 16, 20$  and inverse temperatures  $\beta t = 4, 6, 8$ . Note that  $W_A + W_B = 2L$  such that at  $n = 8$  our largest simulations have 960 sites at an effective inverse temperature  $n\beta t = 64$ . All our simulations are carried out at a finite imaginary time step  $\Delta\tau t = 0.1$ . In Fig. 3 we concentrate on the time reversal symmetric momentum  $k = \pi$  and orbital corresponding to the edge of the cut,  $m = 1$ . Since particle hole symmetry is present in the model, the Dirac cone is pinned at the fermi energy. Thereby a signature of the topological phase, is a non-

decaying single particle entanglement Green function as a function of the replica time  $\tau_E$ . At  $U/t = 5$  we have considered various temperatures and values of  $W_A$ . As apparent, as a function of increasing  $W_A$  and thereby decreasing  $W_B$ ,  $G_{1,1}^E(\pi, \tau_E)$  decays more quickly. This may be assigned to edge-edge correlations across the  $B$  subsystem. The phase transition is triggered by the onset of magnetic correlations which at  $T = 0$  develop long range order beyond  $U_c$  thereby breaking time reversal symmetry. As a consequence, enhancing the temperature will reduced the magnetic correlation length, stabilize the topological state and show a less pronounced decay in  $G_{1,1}^E(\pi, \tau_E)$ .

To obtain a better overview of the data, we can define an entanglement spectral function by analytical continuation of the replica time data:

$$G_{m,m}^E(k, \tau_E) = \frac{1}{\pi} \int d\omega \frac{e^{-\tau_E \omega}}{1 + e^{-\tau_E \omega}} A_{m,m}^E(k, \omega). \quad (43)$$

To carry out this step, we have used the stochastic Maximum Entropy approach [36, 37]. Our results are plotted in Fig. 4. As apparent below  $U_c/t = 5.71(2)$  we observe a single Dirac cone and beyond the phase transition a gap in the entanglement spectrum opens.

The gap in the entanglement spectral function stems from the onset of spin-spin correlations. The equal time spin-spin correlations of the entanglement Hamiltonian can be computed from

$$\langle \hat{S}_{q,m}^x \hat{S}_{-q,m'}^x \rangle_A \equiv \frac{\text{Tr} [\hat{\rho}_A^n \hat{S}_{q,m}^x \hat{S}_{-q,m'}^x]}{\text{Tr} [\hat{\rho}_A^n]} \quad (44)$$

with  $\hat{S}_{q,m}^x = \frac{1}{2\sqrt{L}} \sum_{i_x} e^{iqi_x} \hat{\mathbf{a}}_{(i_x, m)}^\dagger \sigma_x \hat{\mathbf{a}}_{(i_x, m)}$  corresponding to a partial Fourier transformation of the x-component of the spin-operator. As apparent from Fig. 5 a sharp peak at  $q = \pi$  emerges beyond the transition at  $U_c/t = 5.71(2)$

## V. CONCLUSION

In this article we have shown that the two methods put forward to compute the  $n^{\text{th}}$  Renyi entropies in determinant QMC methods for fermions are in essence identical. Starting with the replica scheme proposed in [15, 16] and adapted to determinant [17] and continuous time [18] QMC, we can derive the free fermion or gaussian approach put forward by Grover [19]. The two methods differ in the sampling strategy. The gaussian approach samples  $n$  independent replicas and correlations between the replicas are taken into account by re-weighting. The swap algorithm formulates the QMC in an extended Hilbert space thereby explicitly sampling correlations between replicas. The mapping between both methods shows how to formulate numerical simulations to access entanglement spectra at strong coupling by carrying out a standard simulation within the extended Hilbert space of subsystem  $A$  and  $n$  replicas of subsystem  $B$  albeit with a time dependent Hamiltonian. In contrast to our former approach described in [22] the present formulation does not suffer from uncontrollable fluctuations in the strong coupling regime. We were able to study aspects of the entanglement spectrum in the correlation driven quantum phase transition between a topological insulator and quantum antiferromagnetic as realized in the Kane-Mele Hubbard model. The present formulation is numerically expensive since the total number of sites scales as  $N_A + nN_B$  where  $n$  corresponds to the number of replicas and  $N_A$  ( $N_B$ ) the number of sites in subsystems  $A$  ( $B$ ). The structure of the imaginary time evolution allows for many optimization strategies. Nevertheless, the overall computational effort scales as  $n\beta(N_A + nN_B)^3$ . Our approach to compute the entanglement spectrum is not specific to simulations of fermionic systems in the realm of determinant QMC methods. In fact it can be adapted to bosonic systems within, for example, the SSE [34] approach. Since these methods have a very favorable scaling,  $n\beta(N_A + nN_B)$ , introducing many replicas is not as expensive as for fermions.

I would like to thank T. Lang and F. Parisen Toldin for many invaluable discussions, and P. Bröcker, T. Grover and Lei Wang for comments. We thank the LRZ-München and the Jülich Supercomputing center for generous allocation of CPU time. Financial support from the DFG grant AS120/9-1 is acknowledged.

- 
- [1] L. Amico, R. Fazio, A. Osterloh, and V. Vedral, Rev. Mod. Phys. **80**, 517 (2008).
  - [2] J. Eisert, M. Cramer, and M. B. Plenio, Rev. Mod. Phys. **82**, 277 (2010).
  - [3] M. Levin and X.-G. Wen, Phys. Rev. Lett. **96**, 110405 (2006).
  - [4] A. Kitaev and J. Preskill, Phys. Rev. Lett. **96**, 110404 (2006).
  - [5] S. V. Isakov, M. B. Hastings, and R. G. Melko, Nature

- Phys. **7**, 772 (2011).
- [6] P. Calabrese and J. Cardy, Journal of Statistical Mechanics: Theory and Experiment **2004**, P06002 (2004).
- [7] H. Li and F. D. M. Haldane, Phys. Rev. Lett. **101**, 010504 (2008).
- [8] A. M. Läuchli, E. J. Bergholtz, J. Suorsa, and M. Haque, Phys. Rev. Lett. **104**, 156404 (2010).
- [9] R. Thomale, A. Sterdyniak, N. Regnault, and B. A. Bernevig, Phys. Rev. Lett. **104**, 180502 (2010).

- [10] X.-L. Qi, H. Katsura, and A. W. W. Ludwig, Phys. Rev. Lett. **108**, 196402 (2012).
- [11] L. Fidkowski, Phys. Rev. Lett. **104**, 130502 (2010).
- [12] A. M. Turner, Y. Zhang, and A. Vishwanath, Phys. Rev. B **82**, 241102 (2010).
- [13] F. Kolley, S. Depenbrock, I. McCulloch, U. Schollwöck, and V. Alba, Phys. Rev. B **88**, 144426 ((2013)).
- [14] A. Chandran, V. Khemani, and L. Sondhi, S. Phys. Rev. Lett. **113**, 060501 (2014).
- [15] M. B. Hastings, I. González, A. B. Kallin, and R. G. Melko, Phys. Rev. Lett. **104**, 157201 (2010).
- [16] S. Humeniuk and T. Roscilde, Phys. Rev. B **86**, 235116 (2012).
- [17] P. Broecker and S. Trebst, Journal of Statistical Mechanics: Theory and Experiment **2014**, P08015 (2014).
- [18] L. Wang and M. Troyer, Phys. Rev. Lett. **113**, 110401 (2014).
- [19] T. Grover, Phys. Rev. Lett. **111**, 130402 (2013).
- [20] R. Blankenbecler, D. J. Scalapino, and R. L. Sugar, Phys. Rev. D **24**, 2278 (1981).
- [21] I. Peschel, Journal of Physics A: Mathematical and General **36**, L205 (2003).
- [22] F. F. Assaad, T. C. Lang, and F. Parisen Toldin, Phys. Rev. B **89**, 125121 (2014).
- [23] C. L. Kane and E. J. Mele, Phys. Rev. Lett. **95**, 226801 (2005).
- [24] C. L. Kane and E. J. Mele, Phys. Rev. Lett. **95**, 146802 (2005).
- [25] M. Hohenadler and F. F. Assaad, Journal of Physics: Condensed Matter **25**, 143201 (2013).
- [26] M. Hohenadler, T. C. Lang, and F. F. Assaad, Phys. Rev. Lett. **106**, 100403 (2011).
- [27] M. Hohenadler, Z. Y. Meng, T. C. Lang, S. Wessel, A. Muramatsu, and F. F. Assaad, Phys. Rev. B **85**, 115132 (2012).
- [28] F. F. Assaad, M. Bercx, and M. Hohenadler, Phys. Rev. X **3**, 011015 (2013).
- [29] S. White, D. Scalapino, R. Sugar, E. Loh, J. Gubernatis, and R. Scalettar, Phys. Rev. B **40**, 506 (1989).
- [30] F. F. Assaad, Phys. Rev. B **78**, 155124 (2008).
- [31] J. Hirsch, Phys. Rev. B **28**, 4059 (1983).
- [32] D. Zheng, G.-M. Zhang, and C. Wu, Phys. Rev. B **84**, 205121 (2011).
- [33] F. Assaad and H. Evertz, in *Computational Many-Particle Physics*, Vol. 739 of *Lecture Notes in Physics*, edited by H. Fehske, R. Schneider, and A. Weiße (Springer, Berlin Heidelberg, 2008), pp. 277–356.
- [34] O. Syljuåsen and A. Sandvik, Phys. Rev. E **66**, 046701 (2002).
- [35] F. P. Toldin, M. Hohenadler, F. F. Assaad, and I. F. Herbut, arXiv:1411.2502 (2014).
- [36] A. Sandvik, Phys. Rev. B **57**, 10287 (1998).
- [37] K. S. D. Beach, arXiv:0403055 (2004).